Cambridge University Press
978-1-605-11385-2 - Materials Research Society Symposium Proceedings Volume 1408: Functional Nanowires and Nanotubes
Editors Anna Fontcuberta i Morral, Kornelius Nielsch, Heiner Linke, Hyunjung Shin and Li Shi
Excerpt
More information

Optical Properties

Mater. Res. Soc. Symp. Proc. Vol. 1408 © 2012 Materials Research Society
DOI: 10.1557/opl.2012.30

Composition and Size Effects on the Optical Properties of Isolated Silicon-Germanium Nanowires

Houssem Kallel [1,2,3], Abdallah Chehaidar [3], Arnaud Arbouet [1,2], Thierry Baron[4], Alexis Potié[4], Bassem Salem[4], and Vincent Paillard [1,2]

[1] Université Paul Sabatier, Université de Toulouse, 118 route de Narbonne, 31062 Toulouse cedex 9, France.
[2] CEMES-CNRS, 29 rue Jeanne Marvig, 31055 Toulouse Cedex 4, France.
[3] Département de Physique, Faculté des Sciences de Sfax, Université de Sfax, B.P. 1171, 3000 Sfax, Tunisie.
[4] LTM, CNRS-CEA-LETI, 17 rue des Martyrs, 38054 Grenoble cedex 9, France.

ABSTRACT

Silicon and Germanium nanowires (NWs) have shown a strong ability to enhance both the absorption and scattering of light. Tailoring the optical properties of Si or Ge NWs can be obtained by adjusting the nanowire diameter. Another parameter that can be used is the chemical composition of silicon-germanium ($Si_{1-x}Ge_x$-NWs) alloys. In this work, we perform a numerical study on the optical properties of single $Si_{1-x}Ge_x$-NWs based on the Lorenz-Mie theory. The effects of Ge composition, light polarization and angle of incidence on the nanowire optical properties are investigated.

INTRODUCTION

Semiconductor nanowires are promising novel materials for the next-generation of nano-electronics CMOS transistors, as well as for photovoltaic devices such as photodetectors and solar cells. Among all semiconducting nanostructures, silicon nanowires are nowadays the most studied because of the supremacy of silicon in CMOS technology or low cost solar cells [1-3]. Compared to their bulk counterparts, they show an elastic light scattering enhancement, Raman efficiency enhancement, or increased photoconductivity adjustable by tuning of nanowire diameter. These phenomena are due to morphology-dependent resonances so-called Mie resonances [4-10].

Some theoretical and experimental studies of the optical properties have been performed on pure silicon [4-7] or germanium nanowires [8-10]. The results showed a branched enhancement of absorption and/or scattering resulting from multiple wave interferences inside nanowires of diameters above a given wavelength threshold, and an apparently conventional behavior dominated by direct electronic transitions below this threshold.

For pure Si-NWs or Ge-NWs, the resonance phenomena, leading to electric-field enhancement, occur in a limited spectral region. We propose in this paper, a theoretical study on the optical properties of individual $Si_{1-x}Ge_x$ NWs, which offer the chemical composition x as supplementary tunable parameter. Our calculations show that this parameter leads to high efficiencies over the whole wavelength range of sunlight from near ultraviolet to near infrared.

THEORY

We used the Lorenz-Mie theory [11] applied to the geometry of a nanowire which is described as an infinitely long cylinder of radius *a*, immersed in vacuum, as illustrated schematically in Fig. 1. The plane of incidence is defined by the incident wave vector and the nanowire axis, and ξ is the incidence angle.

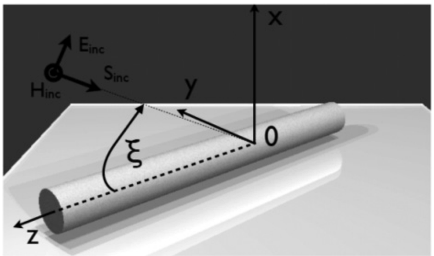

Figure 1- Schematic geometry of light scattering by an infinite cylinder

The calculation is carried out within the linear, homogenous, isotropic scattering medium assumption. In the framework of this theory, the electromagnetic field (**E**, **H**) are solutions of the vector wave equation:

$$\Delta\mathbf{E} + k^2\mathbf{E} = \mathbf{0} \;\text{ and }\; \Delta\mathbf{H} + k^2\mathbf{H} = \mathbf{0} \quad (1)$$

The electromagnetic fields are expanded on the basis of the vector cylindrical harmonics $\mathbf{M}_n$ and $\mathbf{N}_n$ defined by:

$$\mathbf{M}_n = \nabla \times (\hat{u}_z \psi_n) \;\text{ and }\; \mathbf{N}_n = \frac{\nabla \times \mathbf{M}_n}{k} \quad (2)$$

where ψ_n , the solutions of the scalar wave equation, are given by the relation:

$$\psi_n(r,\theta,z) = R_n(r)e^{in\theta}e^{-ik\cos\xi\, z} \quad (3)$$

in which R_n are solutions of the radial Bessel equation. For incident and internal fields $R_n(r) = J_n(kr)$, the Bessel functions of the first kind, while for scattered fields $R_n(r) = H_n^{(1)}(kr)$, the Hankel function of the first kind. From the continuity of the tangential field components at the nanowire-vacuum interface, $r = a$, the expansion coefficients of the scattered field are derived. For the two independent states of polarization of the incident light, transverse magnetic (TM) and transverse electric (TE), these coefficients are given by:

$$a_n = \frac{C_nV_n - B_nD_n}{W_nV_n + i\,D_n^2} \;\text{ and }\; b_n = \frac{W_nB_n + i\,C_n D_n}{W_nV_n + i\,D_n^2} \qquad \text{For TM mode}$$

$$a_n = -\frac{A_nV_n - i\,C_n D_n}{W_nV_n + i\,D_n^2} \;\text{ and }\; b_n = -i\frac{C_nW_n + A_nD_n}{W_nV_n + i\,D_n^2} \qquad \text{For TE mode}$$

with

$$\begin{aligned}
A_n &= i\Omega\sin\xi\,[\Omega\sin\xi\, J_n'(\eta) J_n(\Omega\sin\xi) - \eta\, J_n(\eta)\, J_n'(\Omega\sin\xi)],\\
B_n &= \Omega\sin\xi\,[m^2\Omega\sin\xi\, J_n'(\eta)\, J_n(\Omega\sin\xi) - \eta\, J_n(\eta)\, J_n'(\Omega\sin\xi)],\\
C_n &= n\cos\xi\ \eta\ J_n(\eta) J_n(\Omega\sin\xi)\left(\frac{\Omega^2\sin^2\xi}{\eta^2} - 1\right),\\
D_n &= n\cos\xi\ \eta\ J_n(\eta)\, H_n^{(1)}(\Omega\sin\xi)\left(\frac{\Omega^2\sin^2\xi}{\eta^2} - 1\right),\\
V_n &= \Omega\sin\xi\,[m^2\Omega\sin\xi\, J_n'(\eta)\, H_n^{(1)}(\Omega\sin\xi) - \eta\, J_n(\eta) H_n^{(1)'}(\Omega\sin\xi)],\\
W_n &= i\Omega\sin\xi\,[\eta\, J_n(\eta)\, H_n^{(1)'}(\Omega\sin\xi) - \Omega\sin\xi\, J_n(\eta)\, H_n^{(1)}(\Omega\sin\xi)],
\end{aligned}$$

where $\Omega = \frac{2\pi a}{\lambda}$ is the size parameter, $\eta = \Omega\sqrt{m^2 - \cos^2\xi}$ and m is the NW complex refractive index. The ability of nanowires to absorb or scatter incident light can be characterized by the absorption and scattering efficiencies, Q_{sca} and Q_{abs}, expressed as follows:

$$Q_{sca}^{TM} = \frac{2}{\Omega}\left[|b_0|^2 + 2\sum_{n=1}^{\infty}|b_n|^2 + |a_n|^2\right]$$

$$Q_{sca}^{TE} = \frac{2}{\Omega}\left[|a_0|^2 + 2\sum_{n=1}^{\infty}|a_n|^2 + |b_n|^2\right]$$

$$Q_{abs}^{TM} = \frac{2}{\Omega}\,\mathfrak{Re}\left[b_0 + 2\sum_{n=1}^{\infty} b_n\right] - Q_{sca}^{TM}$$

$$Q_{abs}^{TE} = \frac{2}{\Omega}\,\mathfrak{Re}\left[a_0 + 2\sum_{n=1}^{\infty} a_n\right] - Q_{sca}^{TE}$$

The unpolarized (UP) light configuration corresponds to the average of TE and TM modes, which gives for the efficiencies: $Q_{sca,abs}^{UP} = \frac{1}{2}(Q_{sca,abs}^{TM} + Q_{sca,abs}^{TE})$. In the following calculations, the $Si_{1-x}Ge_x$ NW complex refractive index was assumed to be that of its relaxed bulk counterpart [12,13] irrespective of the NW diameter value.

RESULTS

The computed efficiencies, Q_{abs} and Q_{sca}, in normal incidence (ξ=90°) for unpolarized incident light are reported in Fig. 2 for pure silicon, pure germanium and three $Si_{1-x}Ge_x$ alloy NWs with diameters ranging from 2 to 250 nm. The results obtained for Si and Ge NWs are in good agreement with those published by Brönstrup *et al.* and Cao *et al.* [5-10].

Branched resonances, appearing in the map, correspond to highly confined modes, also identified as leaky mode resonances in optical fibers and other dielectric resonators [8]. The branched resonance distribution shifts towards the red part of the spectrum with increasing alloy composition *x*. Indeed, this corresponds to the redshift of the maximum of the refractive index (real part of *m*). The high refractive index value allows the trapping of light in $Si_{1-x}Ge_x$ nanowires, since the wavelength of light in vacuum, ranging from 300 to 1200 nm, diminishes

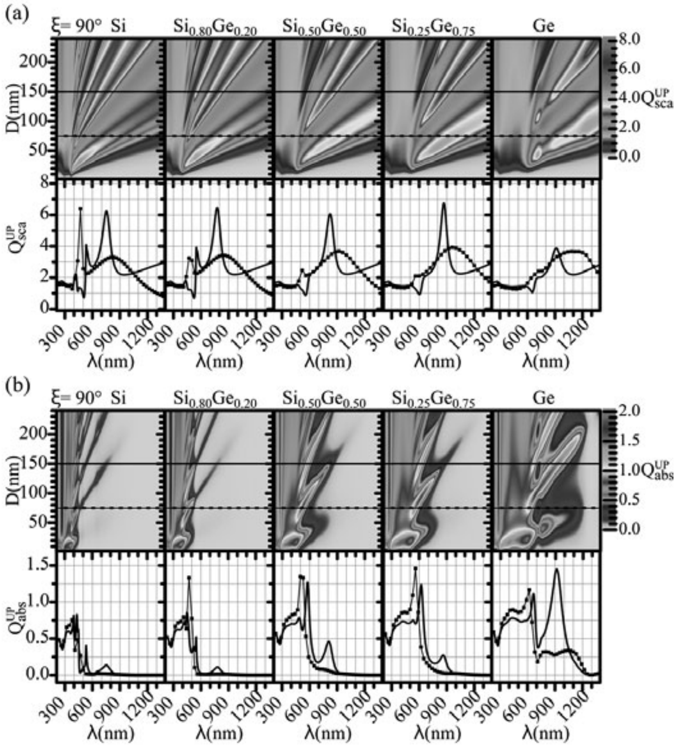

Figure 2- Unpolarized scattering (a) and absorption efficiencies (b) in $Si_{1-x}Ge_x$ alloy nanowires as a function of the wavelength and the nanowire diameter: (top) Two-dimensional map and (bottom) efficiencies spectra for nanowire diameters 150 nm (solid line) and 75 nm (thin solid line with filled squares).

inside the NW and becomes of the same order of magnitude as the NW diameter. A wavelength threshold in the scattering efficiency, below which the branches disappear, can be noticed. For the absorption efficiency, a NW diameter cutoff is imposed in addition, below which Q_{abs} can reach high values. These two characteristics can be correlated with the penetration depth of the light in the nanowires as function of the wavelength. As expected, they show a wavelength redshift with increasing Ge composition in $Si_{1-x}Ge_x$ alloy nanowires. Thinner NWs with diameters equivalent to the light penetration depth exhibit higher Q_{abs} due to the possible cumulated effects of both direct electronic transitions and optical resonances. The maximum of Q_{abs} is highly localized in Si, corresponding to the E'_0 and E_1 transitions located at 364 and 295 nm, respectively. The Q_{abs} maximum region is spread over a broader range of wavelengths with increasing concentration of Ge, according to the degeneracy lifting of E_0', E_1, $E_1 + \Delta_1$, $E_0 + \Delta_0$ [14].

Thus, it is obvious that the specific optical properties of $Si_{1-x}Ge_x$ NWs are of great interest for the optimization of both light scattering and absorption in solar cells or photodetectors. They are also very important for enhanced Raman scattering from and by nanowires. The benefit of sharp Mie resonances in Raman scattering was illustrated recently by Poborchii et al. [15], who investigated Si NWs of diameters less than 20 nm excited by a resonant laser line at 363.8 nm. Cao *et al.* showed similar Raman efficiency enhancement using non-resonant visible excitations, but for thicker nanowires [5]. Therefore, using $Si_{1-x}Ge_x$ alloys should allow light absorption and scattering engineering, reaching high Q_{abs} and Q_{sca} values over a wide wavelength range but within a limited nanowire diameter range.

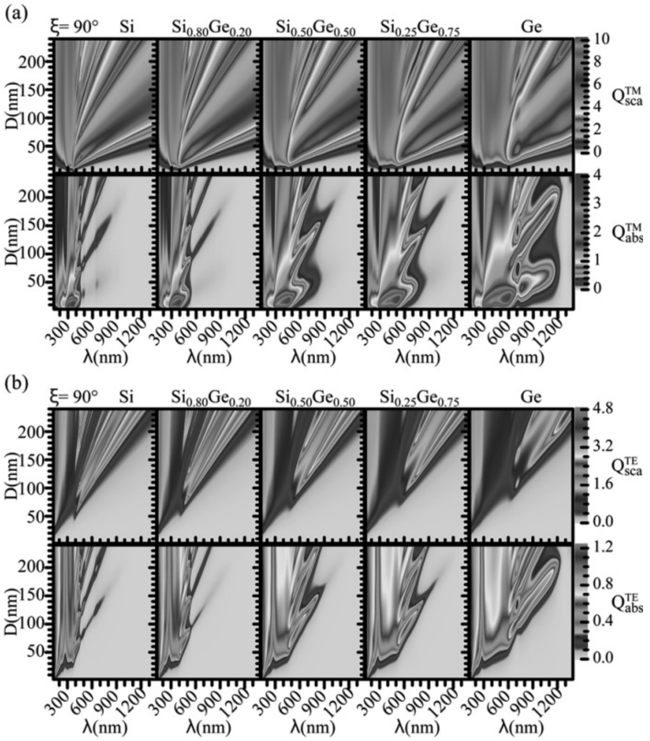

Figure 3- Absorption and scattering efficiencies as function of NW diameter and incident wavelength for different compositions *x* of Ge under normal incidence illumination and for polarized incident light: (a) TM mode and (b) TE mode.

The effect of light polarization on the scattering and absorption efficiencies of $Si_{1-x}Ge_x$ NWs is illustrated in Fig. 3 for normal incidence illumination. As can be noted from this figure, the maxima of both Q_{abs} and Q_{sca} under TM polarization are noticeably greater than those achieved under TE polarization [Fig. 2(a) vs Fig. 2(b)]. This can be attributed to the higher number of dipoles excited when the electric field is aligned with the NW axis (TM mode). In agreement with Fig. 2(a) where Q_{abs} reaches 400%, the enhanced Raman efficiency was clearly evidenced in the TM configuration for Si NWs of diameters less than 20 nm [15].

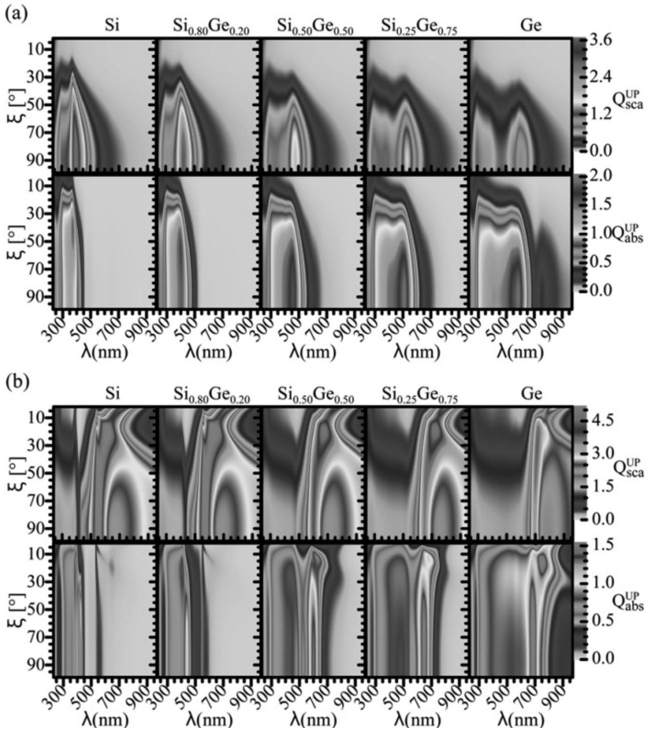

Figure 4- Unpolarized absorption and scattering efficiencies for two nanowire diameters and different alloy compositions *x* as function of the incidence angle ξ and the incident wavelength: (a) D_1=20 nm (c) D_2= 100 nm.

In Fig. 4, we present Q_{abs} and Q_{sca} as function of the angle of incidence ξ for different concentrations of Ge and for two diameters (D_1= 20 nm and D_2= 100 nm). For the smallest diameter D_1, there is sharp transition for angles smaller than 40° in the plot of Q_{sca} or 30° in the plot of Q_{abs}. These efficiencies do not change a lot while decreasing incident angles from normal incidence down to the above mentioned limits, and are constant and close to zero beyond these limits. The behavior is different in the case of the larger diameter D_2, where the scattering efficiency can be still high at low incidence angle, but for slightly different wavelengths. For instance in the case of D_2, the Q_{sca} maximum at small incidence angles (about 450-500% at 20°) is red shifted by about 50 nm compared to the same Q_{sca} maximum at larger incidence angles (about 450-500% from 35° to 90°), over the whole range of ξ. Thus, the scattering spectrum (or the color) of a NW excited by a wide range of wavevectors including low incidence angles, should not be different from the color of the same nanowire under normal incidence if its diameter is close to D_1 = 20 nm. However, the observed color of larger nanowires would be different depending on the incidence angle distribution.

CONCLUSION

The scattering and absorption efficiencies of single $Si_{1-x}Ge_x$ nanowires have been calculated and their dependence on the NW diameter, alloy composition, light polarization and angle of incidence has been investigated using the Lorentz-Mie theory. We showed that scattering and absorption of light can be tuned via the alloy composition in addition to the nanowire diameter. High values of either Q_{sca} or Q_{abs} can be obtained over an extended wavelength range from near-UV to near-IR covering most of the sunlight spectrum. Highest efficiencies can be achieved with transverse magnetic polarization under normal incidence illumination.

ACKNOWLEDGMENTS

HK and VP would like to thank French Ministry of Foreign Office, French Embassy in Tunis, and Université Paul Sabatier for financial support.

REFERENCES

1. Y. Li, F. Qian, J. Xiang and C. M. Lieber, Mater. Today **8**, 18–27 (2006).
2. P. Yang, R. Yang, and M. Fardi, Nanolett. **10**, 1529–1536 (2010).
3. M. D. Kelzenberg, S. W. Boettcher, J. A. Petykiewicz, D. B. Turner-Evans, M. C. Putnam, E. L. Warren, J. M. Spurgeon, R. M. Briggs, N.S. Lewis and H. A. Atwater, Nature Mat. **9,** 239–244 (2010).
4. G.-H. Ding, C. T. Chan, Z. Q. Zhang and P. Sheng, Phys. Rev. B **71**, 205302 (2005).
5. L. Cao, B. Nabet and J. E. Spanier, Phys. Rev. Lett. **96**, 157402 (2006).
6. L. Cao, P. Fan, A. P. Vasudev, J. S. White, Z. Yu, W. Cai, J. A. Schuller, S. Fan and M. L. Brongersma, NanoLett. **10**, 439–445 (2010).
7. L. Cao, P. Fan, E. S. Barnard, A. M. Brown and M. L. Brongersma, NanoLett. **10**, 2649–2654 (2010).
8. L. Cao, J. S. White, J.-S. Park, J. A. Schuller, B. M. Clemens and M. L. Brongersma, Nature Mat. **8**, 643–647 (2009).
9. L. Cao, J.-S. Park, P. Fan, B. Clemens and M. L. Brongersma,. NanoLett. **10**, 1229–1233 (2010).
10. G. Brönstrup, N. Jahr, C. Leiterer, A. Csaki, W. Fritzsche and S. Christiansen, ACS Nano **4**, 7113–7122 (2010).
11. C. F. Bohren and D. R. Huffman, *in Absorption and Scattering of Light by Small Particles* (John Wiley and Sons, New York, NY, 1998) pp. 194-208.

12. J. Humlíček, M. Garriga, M. I. Alonso and M. J. Cardona, Appl. Phys. **65**, 2827–2832 (1989).
13. J. Humlíček, *in Properties of Silicon Germanium and SiGe:Carbon*, edited by E. Kasper and K. Lyutovich (INSPEC, Institution of Electrical Engineers, London, 2000), pp. 249-259.
14. C. Penn, T. Fromherz and G. Bauer, *in Properties of Silicon Germanium and SiGe:Carbon*, edited by E. Kasper and K. Lyutovich (INSPEC, Institution of Electrical Engineers, London, 2000), pp. 125-134.
15. V. Poborchii, T. Tada, Y. Morita, T. Kanayama and P. I. Geshev, Phys. Rev. B **83**, 153412 (2011).